Testing the parameters of the "universal" Woods-Saxon potential with $B(E2;0_1^+ \rightarrow 2_1^+)$ values and nucleon separation energies

S. Kahane
Joint Institute for Heavy-Ion Research, Oak Ridge, Tennessee 37831
and Nuclear Research Center–Negev, Beer Sheva, Israel

S. Raman
Oak Ridge National Laboratory, Oak Ridge, Tennessee 37831

J. Dudek
Joint Institute for Heavy-Ion Research, Oak Ridge, Tennessee 37831
and University Louis Pasteur, Theoretical Physics Division, 23 rue du Loess, F-67037 Strasbourg CEDEX, France
(Received 14 July 1989)

The idea of "universality" of an average nuclear field introduced earlier has been applied and tested in the calculations of $B(E2;0_1^+ \rightarrow 2_1^+)$ values and nucleon separation energies for nuclei in the $Z \geq 52$, $A \geq 120$ region. Good description is obtained using a single "universal" choice of 12 constants defining the deformed Woods-Saxon nuclear average field.

I. INTRODUCTION

During the whole history of nuclear physics, the existence of approximately 2630 nuclei has been experimentally established, yet this large number corresponds merely to something like 30–40 % of the total number of nuclei expected to exist in nature. Indeed, extrapolations of formulas for the nucleon binding energies give very broad existence limits; it is estimated that 6000–7000 nuclei, most of them short-lived products of various reactions, may, in principle, be produced in a laboratory. Detailed nuclear structure studies have been possible until now only for a relatively small fraction of all known nuclei. For many of them, our knowledge is limited to a few excited states, often without spin and parity identifications. Keeping in mind the necessity of future studies of those often exotic nuclei, both experimental and theoretical methods need specially designed approaches.

One of the most powerful theoretical methods in the physics of nuclear structure is a deformed average field approximation that, supplemented with the Strutinsky[1] energy theorem, provides an extremely useful way of calculating various properties of deformed nuclei.[2] In the Strutinsky approach, the total energy of the nucleus is calculated approximately as a sum:

$$E_{\text{total}}(\text{def}) = E_{\text{macro}}(\text{def}) + E_{\text{micro}}(\text{def}) , \tag{1}$$

where (def) denotes all the deformation degrees of freedom and the macroscopic part $E_{\text{macro}}(\text{def})$ is usually represented by the liquid drop model mass formula.[3] The microscopic part $E_{\text{micro}}(\text{def})$ is often referred to as "quantal" or "shell" energy and is a known function[1] of the single-particle level spectrum $\{\epsilon_\nu(\text{def})\}$:

$$E_{\text{micro}}(\text{def}) = E_{\text{micro}}\{\epsilon_\nu(\text{def})\} . \tag{2}$$

The single-particle levels are, in all practical applications, calculated by solving the one-body Schrödinger equation with the average field Hamiltonian

$$\hat{H} = \hat{H}(\text{def}), \quad \hat{H}\phi_\nu(\hat{x}) = \epsilon_\nu \phi_\nu(\hat{x}) . \tag{3}$$

It thus becomes clear that applicability of this method to very exotic and largely unknown nuclei depends, to a far extent, on the "universality" of the Hamiltonian of Eq. (3). In other words, it is necessary, in this context, to employ an average field that can be expressed in terms of parameters common for (preferably) all nuclei throughout the periodic table (≡ *universal)* so that the corresponding Hamiltonian describes the single-particle properties with satisfactory accuracy.

It has been recently argued[4,5] that the Woods-Saxon potential with the parameters of Ref. 6 can serve well in the "universal" description program formulated above (see also Ref. 7). The correct parametrization of the spin-orbit is extremely important for the correct description of the single-particle level order and of high-spin nuclear phenomena like angular momentum alignment, for progress in understanding Coriolis antipairing effect as a function of spin, etc. Numerous studies have tested this spin-orbit part (cf. references quoted in Ref. 5). By contrast, the parametrization of the central part of the potential has not received satisfactory attention. The procedure used until now was essentially the one adopted from the early Rost[8] study of 1968. It is the purpose of this investigation to provide a global test of the central part of the universal Woods-Saxon field (parametrization of the effective radius and depth of the potential) using the experimental data currently available.

II. UNIVERSAL NUCLEAR AVERAGE FIELD

In the following, the main facts that gave rise to the concept of universality in the context of the nuclear aver-

age field are outlined briefly. For completeness, the average field potential employed in this paper is also explicitly defined.

A. Concept of universality

The microscopic background, within the framework of the Bethe-Goldstone approach, leading from realistic nucleon-nucleon interactions to the average field description of nuclear phenomena was provided many years ago (see, e.g., Ref. 9 and references therein). Although such a theory was an approximation and used mainly in the infinite nuclear matter context, it revealed adequately the main clues supplied by the short-range forces on one hand and the characteristic restricting role of the Pauli principle on the other. More precisely, two main physical elements were introduced in this theory: (1) "realistic" nucleon-nucleon interactions in the Schrödinger-type theory of motion, and (2) the exclusion principle that blocks the scattering into already occupied orbitals. Approximations[9] introduced due to the numerical complexity of the problems justified an alternative name for this theory as an *independent pair approximation.* The Bethe-Goldstone approach thus offered an important step beyond the usual Schrödinger equation treatment of a system of independent particles. The mathematical complexity of this approach, however, permitted numerical solutions only for nucleonic systems of special symmetries, and the conclusions relevant in the context of the average field methods were obtained, strictly speaking, only for infinite nuclear matter. The most important results, whose applicability seem to extend well into the realm of finite nuclei, can be summarized as follows.

The characteristic determinants of the nucleonic motion in an extended nuclear medium are (1) a "hard-core" radius $r_{hc} \approx 0.4$ fm, corresponding to the presence of an extremely strong repulsion at short distances; (2) an effective "free-nucleon" radius $r_v \approx 1.6$ fm, deduced from the characteristic volume $V = 1/\rho_0$ (ρ_0 is the nuclear matter density) available to a nucleon in nuclear matter (or in a heavy nucleus); and, very importantly, (3) a characteristic "healing distance" calculated within the Bethe-Goldstone approach as $h \approx 0.8$ fm such that for relative nucleon-nucleon separations exceeding h the corresponding two-nucleon wave functions resemble essentially those of the free nucleons. The above values for r_v and h implied by nuclear matter calculations give rise, in turn, to the following consequence: in about 85% of the volume available to a nucleon, its motion is essentially free ($V_v/V_h = \frac{4}{3}\pi r_v^3 / \frac{4}{3}\pi r_h^3 \approx 8$).

One therefore arrives at the following formulation of the nuclear structure program. If the nucleonic motion is constrained by a correct surface (correct nuclear shape), the independent-particle approximation should provide a good first approximation to the wave functions (correct within up to $\approx 85\%$ of the nuclear volume); furthermore, the "missing" part of the interaction can be taken care of next, using the concept of residual forces and appropriately designed approximate treatment (e.g., the pairing short-range residual forces and the Bardeen-Cooper-Schrieffer (BCS) theory; the multipole-multipole interaction and the random-phase-approximation (RPA) treatment, etc.).

The hypothesis of the existence of a universal average field arises as a natural outcome of the following line of reasoning. (1) The leading feature of nucleonic motion in an extended medium is, to a first approximation, the manifestation of a noninteracting-particle picture ("free motion" as already discussed). (2) The short range of the attractive nuclear forces permits the simulation of nucleonic confinement within the nuclear volume by a one-body potential with relatively steep "walls." (3) This one-body potential can simultaneously combine the role of confining the motion of the nucleons and the role (via the one-body Schrödinger equation) of providing the quantum mechanical wave functions for noninteracting particles. (4) The successful descriptions of the nucleon-nucleus scattering using the Woods-Saxon form of the potential suggest the physical relevance of this particular form for nuclear structure applications. (5) Numerous experiments clearly show that the nuclear spin-orbit interaction is strong in most nuclei (except in the lightest ones) and the "usual" positions occupied by the so-called "intruder orbitals" are crucial for the shell structure. Therefore, it is inevitable that spin-orbit effects must be included in any successful average field approach. Because the average spin-orbit potential is usually related to the central potential itself via the scalar coupling,[10]

$$V_{so} \approx (\nabla V_{\text{central}} \times \mathbf{p}) \cdot \mathbf{s} \ , \tag{4}$$

it is clear that the geometry of the central part will also determine that of the effective spin-orbit part of the potential. Consequently, the idea of universality should be applicable to both parts. (6) Finally, to win acceptance, the concept of the universal nuclear field (with the Woods-Saxon form as a possible solution) needs to be (and has been) tested on as many nuclei as possible throughout the periodic table.

While numerous previous studies, notably on high-spin behavior, have tested the performance of the spin-orbit term in various nuclear regimes, the optimization of the radius and depth of the central potential has been until now of only limited interest. To proceed with the discussion of these two geometrical aspects, the definition of the potential is recalled next.

B. Definition of the deformed Woods-Saxon field

Calculations reported in this article are restricted to the axially symmetric shapes. The deformed Woods-Saxon potential is defined with the help of the equation of nuclear surface, Σ, which in our application stands for

$$R(\theta) = c(\beta) R_0 [1 + \beta_2 Y_{20}(\cos\theta) + \beta_4 Y_{40}(\cos\theta)] \ , \tag{5}$$

where $R_0 = r_0 A^{1/3}$ and $c(\beta)$ ensures that the volume enclosed by this surface [$\beta \equiv (\beta_2, \beta_4)$] is constant. This deformed surface induces a deformed single-particle potential defined by

$$V(\mathbf{r}) = \bar{V} \{ 1 + \exp[\text{dist}(\mathbf{r}, \beta)/a] \}^{-1} \ , \tag{6}$$

where $\text{dist}(\mathbf{r}, \beta)$ is the distance of a point $\mathbf{r}$ from the nu-

TABLE I. Universal Woods-Saxon parameters

Parameter	Where used	Old value		New value	
		Proton	Neutron	Proton	Neutron
V_0 (MeV)	Eq. (7)	49.6		50.6	
κ	Eq. (7)	0.86		0.86	
r_o (fm)	Eq. (5)	1.275	1.347	1.250	1.320
a (fm)	Eq. (6)	0.70	0.70	0.70	0.70
λ	Eq. (8)	36.0	35.0	36.0	35.0
r_0^{so} (fm)	Eq. (8)	1.320	1.310	1.320	1.310
a^{so} (fm)	Eq. (8)	0.70	0.70	0.70	0.70

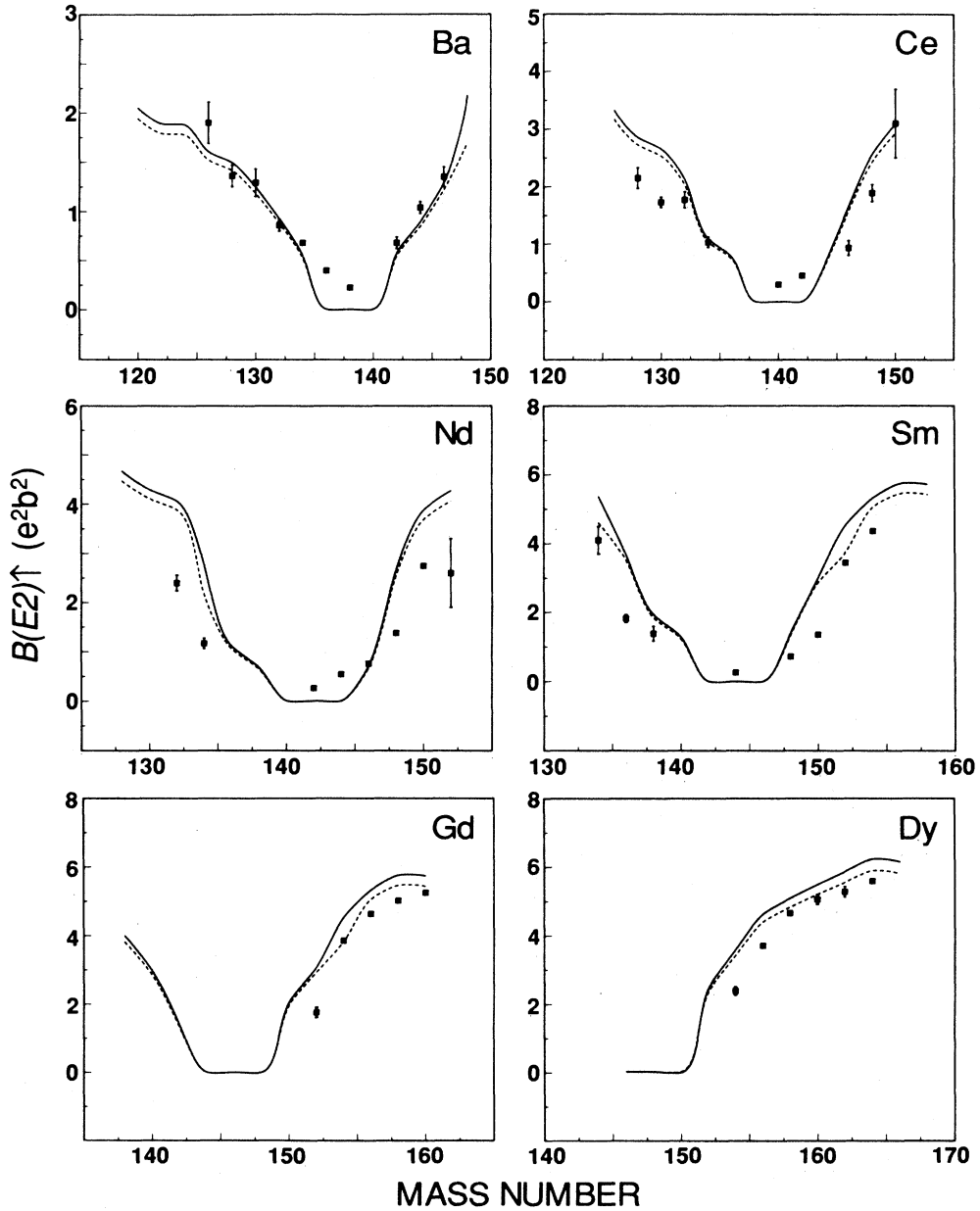

FIG. 1. Comparison between calculated and measured $B(E2)\uparrow$ values for nuclei in the light rare-earth region. The curves connecting the calculated values have been smoothed by the method of rational splines (cubic splines with tension). The solid curve corresponds to the standard parametrization (see Table I) and the dashed curve to the same parametrization except for a 2% reduction in the r_0 value.

clear surface Σ and a is the diffuseness parameter. The depth $\bar{V}$ is parametrized as

$$\bar{V}=V_0\{[1\pm\kappa(N-Z)]/(N+Z)\}\ , \tag{7}$$

the plus sign for protons and minus for neutrons. Because the effective forces acting on the neutrons and protons are, in general, different (the effects of Coulomb forces, the very different numbers of the neutrons as compared to that of the protons, etc.) the corresponding radius and depth constants are also different for the two kinds of particles. (Table I collects all initial values of parameters.) The spin-orbit part of the potential is related to the central part by

$$V_{so}\approx\lambda(\hbar/2Mc)[\nabla V(r)]\cdot(\sigma\times\mathbf{p})\ , \tag{8}$$

where M is the nucleon mass. As argued in Ref. 11, the radius parameters for the central and spin-orbit part of the potential, R_0 and r_{so}, respectively, must be, in general, different (cf. Table I).

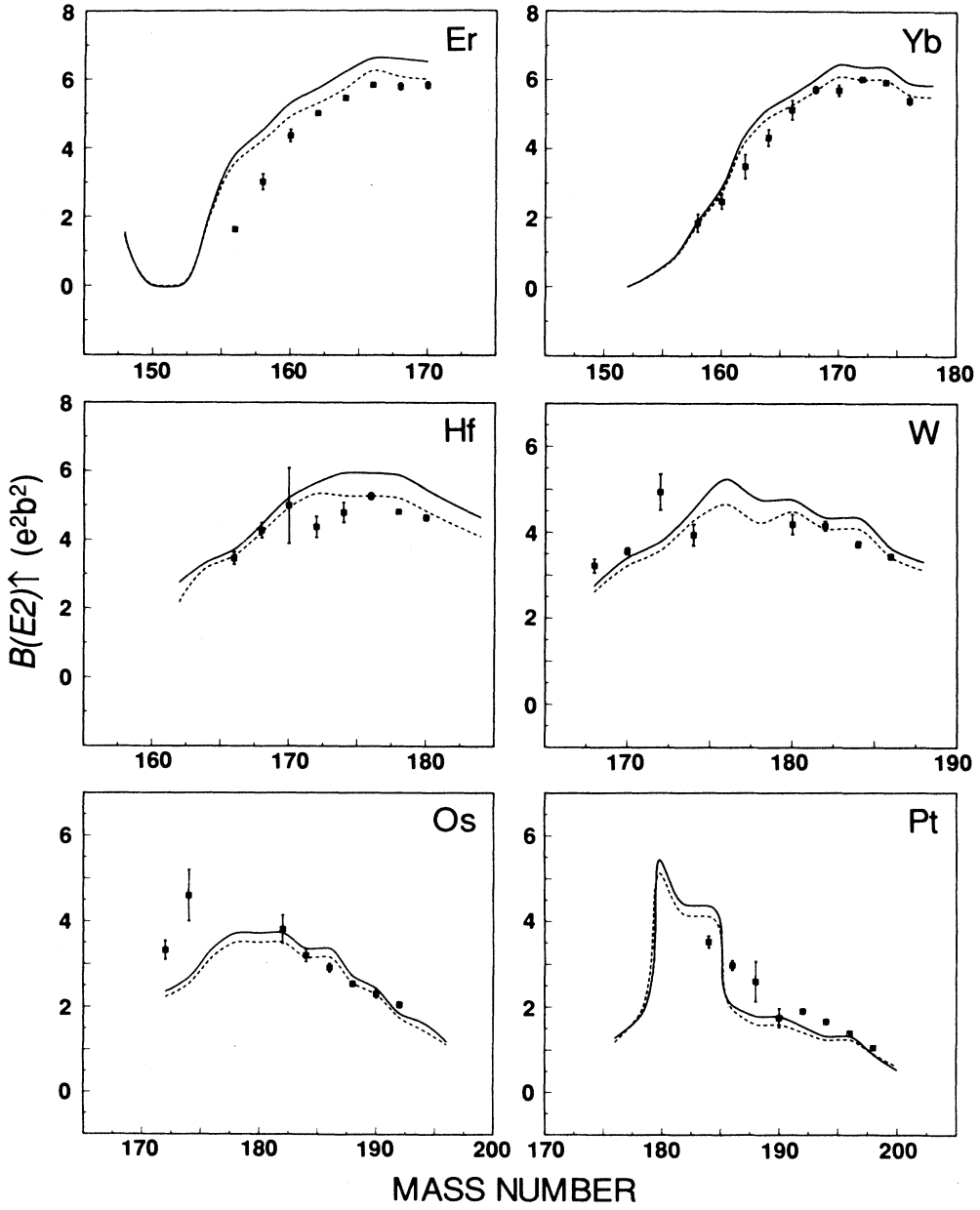

FIG. 2. Comparison between calculated and measured $B(E2)\uparrow$ values for nuclei in the heavy rare-earth region. See caption to Fig. 1 for further details.

III. ANALYSIS OF THE $B(E2;0_1^+ \rightarrow 2_1^+)$ VALUES

The reduced transition probabilities were obtained at the equilibrium deformation from the calculated proton quadrupole moments Q_p via

$$B(E2)\uparrow = \left[\frac{5}{16\pi}\right] Q_p^2(\beta_{2,\mathrm{eq}},\beta_{4,\mathrm{eq}}) \ . \tag{9}$$

Therefore the two-dimensional total energy minimization in the $(\beta_{2,\mathrm{eq}},\beta_{4,\mathrm{eq}})$ plane had to be performed first.

A. Remarks on equilibrium deformations

The single-particle energies and wave functions have been calculated using potential [Eqs. (5)–(8)] for a mesh of β_2 and β_4 values. The mesh extended from

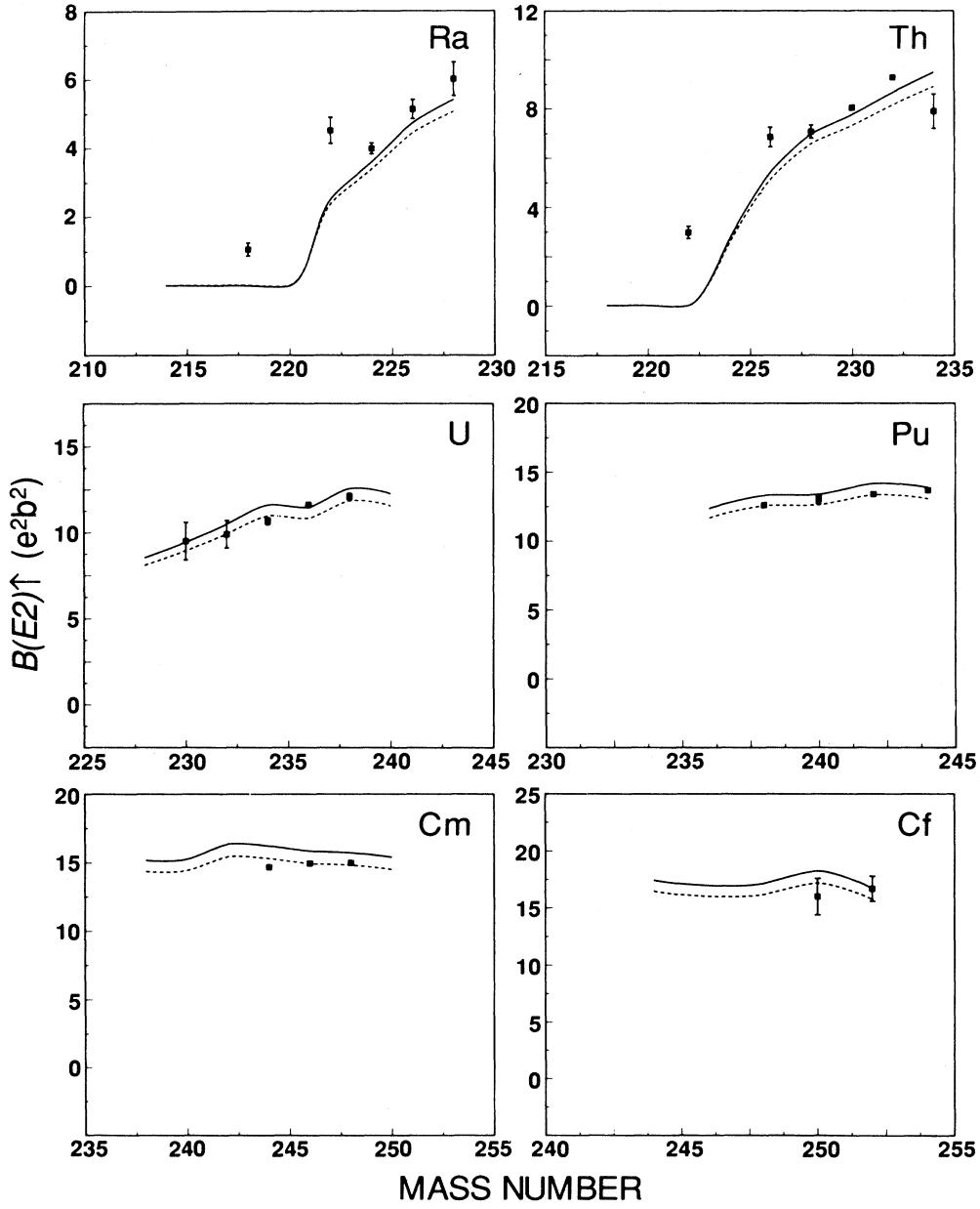

FIG. 3. Comparison between calculated and measured $B(E2)\uparrow$ values for nuclei in the actinide region. See caption to Fig. 1 for further details.

$-0.3 \leq \beta_2 \leq 0.5$ in steps of 0.05 and from $-0.16 \leq \beta_4 \leq 0.16$ in steps of 0.04. This type of mesh calculation becomes time consuming; it is known, however, that this procedure need not be repeated for each and every nucleus. The verified assumption is that the level energies and wave functions of the deformed Woods-Saxon potential vary slowly with Z and N and can be used safely for a number of neighboring nuclei, the nucleons just filling in a different way the same energy levels. Thus the mesh calculations were undertaken only for some central "anchor" nuclei. Specifically, a ^{122}Xe anchor was used for the region from (^{104}Sn to ^{152}Nd); ^{150}Gd for (^{142}Nd to ^{178}Yb); ^{186}Os for (^{162}Hf to ^{206}Hg); ^{210}Po for ^{182}Hg to ^{228}Ra); and ^{238}U for (^{218}Th to ^{254}Fm). The groups of nuclei appearing with two anchors were used to check the assumption made above on the slow (Z,N) dependence.

The total energy was calculated using the macroscopic-microscopic model of Strutinsky [Eq. (1)]. The macroscopic part representing the bulk properties of the nucleus was approximated by the liquid drop model energy of Myers and Swiatecki.[3] The microscopic part describes those properties that depend on the single-particle motion of the individual nucleons. This part is divided into a shell correction term and a contribution coming from a residual pair interaction

$$E_{\text{micro}} = E_{\text{shell}} + E_{\text{pair}} \ . \tag{10}$$

The pairing contribution was calculated as in Ref. 12. The shell energy used in calculating the total energy is

$$E_{\text{shell}} = \sum_{i=1}^{N \text{or} Z} \epsilon_i - \int g(\epsilon) \epsilon \, d\epsilon \ , \tag{11}$$

where ϵ_i are the single-particle energies and $g(\epsilon)$ is the smoothed single-particle level density. [The two Strutinsky parameters entering the definition of $g(\epsilon)$, viz. smoothing parameter γ and smoothing order p were set as follows: $\gamma = 1.2\hbar\omega_0$ and $p=6$, where $\hbar\omega_0 = 41 A^{-1/3}$ MeV; for definitions, see, e.g., Refs. 1 and 2.] The equilibrium deformations were obtained as the point in the (β_2, β_4) plane that minimizes the total energy [see Eq. (1)].

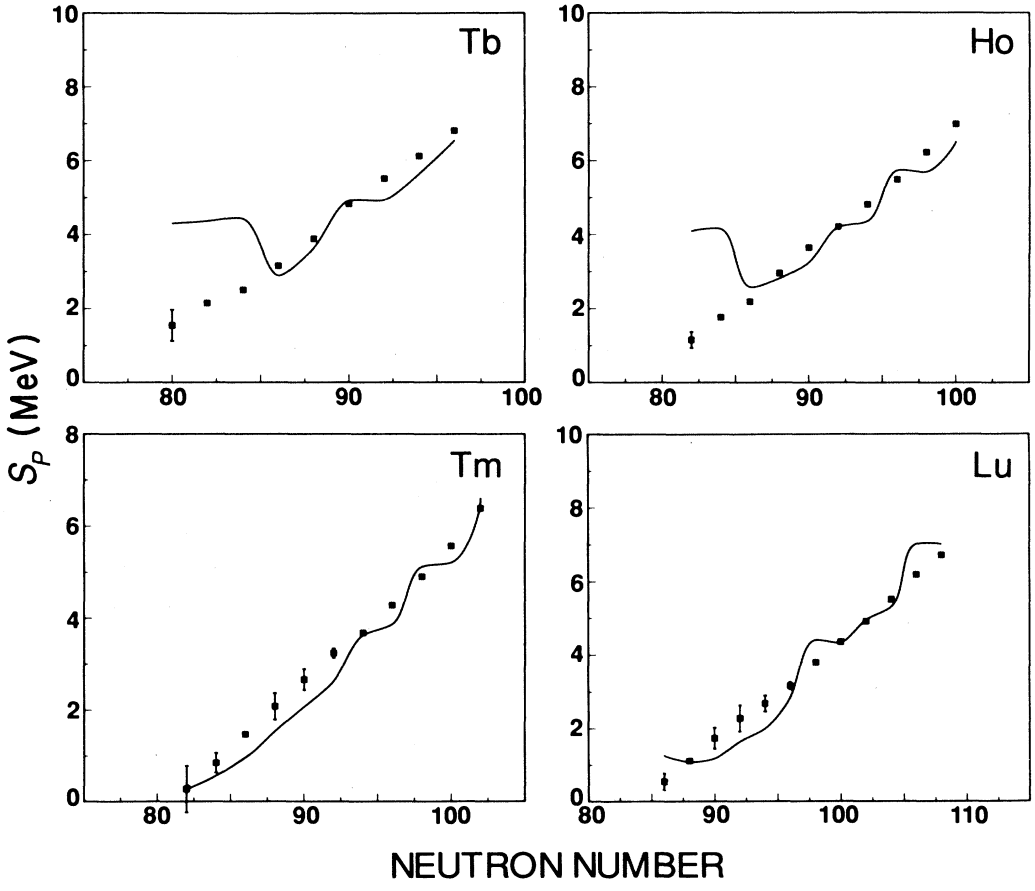

FIG. 4. Comparison between calculated and measured proton separation energies (S_p) for selected rare-earth nuclei. The curves connecting the calculated values have been smoothed by the method of rational splines (cubic splines with tension).

B. Quadrupole moments and $B(E2;0_1^+ \rightarrow 2_1^+)$ values

These equilibrium deformations were then used to calculate single-particle energies, wave functions, and quadrupole moments. The intrinsic quadrupole moment was obtained from

$$Q_p = \sum_{i=1}^{Z/2} q_i \times 2; \quad q_i = \langle i|\hat{Q}_2|i\rangle; \tag{12}$$

and

$$\hat{Q}_2 = e(5/16\pi)^{1/2} r^2 Y'_{20}$$

according to standard notation and definitions. When the pairing interaction is included,

$$Q_p = 2 \sum_{i=1}^{Z} q_i \times v_i^2 , \tag{13}$$

with i running over the proton single-particle states and v_i^2 denoting the occupation coefficient of the ith state. The reduced transition probabilities follow from the approximate Eq. (9).

There are essentially two sets of parameters optimized for the spin-orbit performance that were considered in the current analysis; they are referred to in Ref. 5 as "optimal" and "universal" (for the latter see Ref. 6 and Table I; the former has been discussed in Refs. 5 and 6). Both sets differ in the parametrization of the spin-orbit potential and were checked to provide a good single-particle level order over a broad range of nuclei. The two possible choices are not expected to influence the calculated $B(E2)\uparrow$ values in any significant way; this statement has been also checked here numerically. Therefore, in the following discussions, only the results of the universal parametrization are presented.

An overview of the results obtained is shown in Fig. 1 for the light rare earth, in Fig. 2 for the heavy rare earth, and in Fig. 3 for the actinide nuclei. Theoretical results correspond to the standard universal parametrization (solid lines) and, in order to show the sensitivity to the most important parametrical dependence (i.e., dependence on the proton radius parameter), also to the slightly reduced (98% of the original value) r_0 value (dashed lines). This comparison shows that, while for the actinide nuclei the reduction in r_0 causes no particular improve-

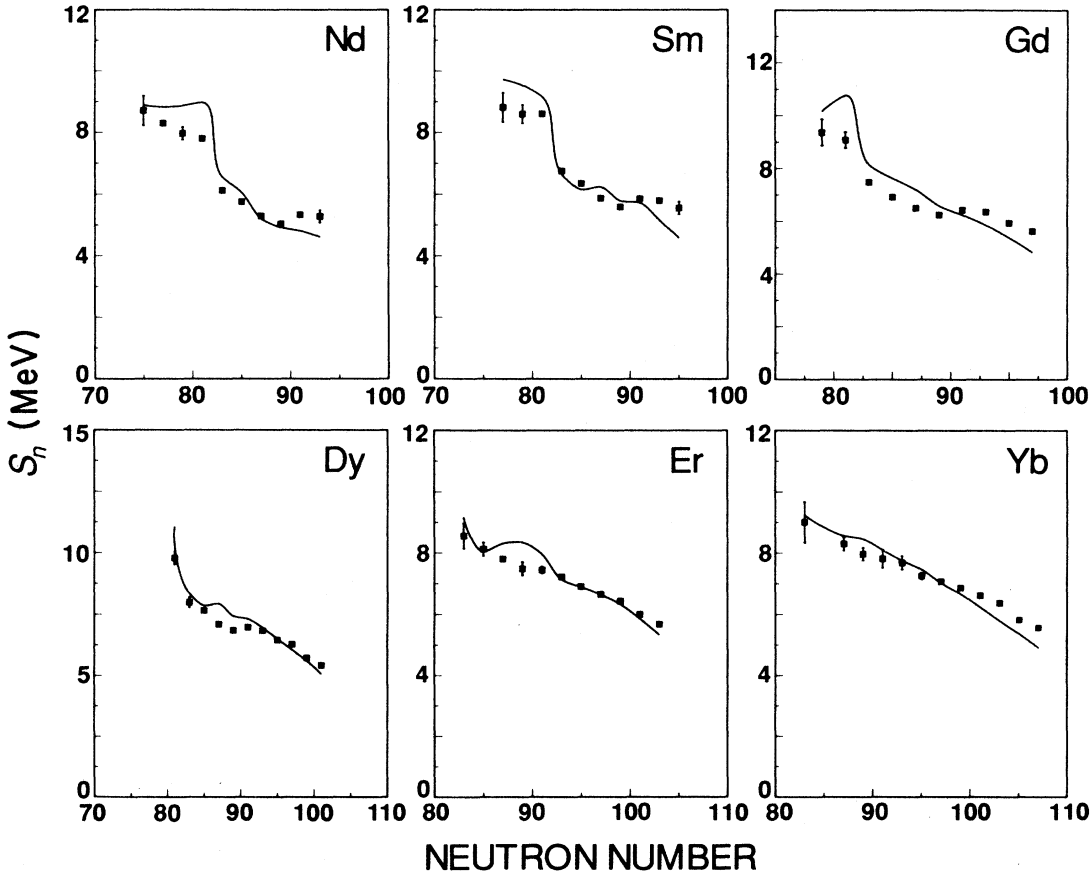

FIG. 5. Similar to Fig. 4, but for the neutron separation energies (S_n) of selected rare-earth nuclei.

ment in the agreement with the experimental data,[13] for the rare-earth nuclei there is indeed a systematic improvement.

Even though the overall agreement appears to be very good, one has to keep in mind the limitations of the simple expression, Eq. (9), used here. Firstly, the transition quadrupole moments were replaced by the static ones where initial (ket) and final (bra) states are identical. Secondly, the standard formula [see Eq. (9)] applied does not take into account the effect of quantal fluctuations on the quadrupole moments (compare with a discussion of this problem in Ref. 14). The influence of shape oscillations (or the zero-point motion) on the compared quantities has been neglected. This last effect has been estimated to be negligible for well-deformed nuclei (Ref. 14) but has some bearing on the results for near-spherical nuclei.

IV. ANALYSIS OF THE NUCLEON SEPARATION ENERGIES

A finite average field, like the deformed Woods-Saxon potential discussed in this paper, can also provide simple estimates for the nucleon binding in nuclei and its dependence on N and Z. One has to keep in mind though that the nucleon separation energies extracted from experiment and identified as binding may generally be influenced by more complex interaction effects than just an average nuclear field. With this precaution, one can view the following comparison between the calculated nucleon binding energies on one hand and the empirical separation energies (taken from the 1983 atomic mass evaluation[15]) on the other as a simplified test for, first of all, the dependence of the central nuclear potential on the effective potential depth [defined by Eq. (7)] and the radius parameters $(r_0)_{\pi,\nu}$. It is emphasized again that, in the spirit of the universal realization of the field, the parameters V_0, κ, $(r_0)_\pi$, and $(r_0)_\nu$, like all other parameters of the potential, are kept constant for all the nuclei considered.

In the following, the proton separation energies of the odd-Z, even-N nuclei and the neutron separation energies of the even-Z, odd-N nuclei will be discussed. The corresponding even-Z, even-N core nuclei were the same as those chosen for the calculation off the $B(E2)\uparrow$ values; similarly, the equilibrium deformation parameters for odd nuclei were assumed to be the same as those for the respective even-even core nuclei. Such an assumption is reasonable because, in most of the cases, these parameters do not vary sharply with Z and N.

Nucleon emission is a complex process which, as already mentioned, involves not only the notions of the independent-particle model but also residual interactions. In particular, the matrix elements between the initial bound state and the final resonance state influence the emission probability. In the current context, there are two simple estimates that one can obtain of the global behavior of the separation energies as a function of Z and N. The most extreme approximation ignores all possible interactions except those already represented by the average field. The separation energy is then given by the difference

$$S=\epsilon_{\text{resonl}}-\epsilon_{\text{occupl}}\ , \tag{14}$$

where ϵ_{resonl} denotes the energy of the first unbound (resonance) state and ϵ_{occupl} denotes the last occupied Woods-Saxon level. The second simplified approach, which is also straightforward, is to consider the nuclear system as interacting via the pairing forces. In such a case, the simple (pairing) model of the residual interactions imposes a different definition of the excitation energy. The separation energy is now given by

$$S=E(\epsilon_{\text{resonl}})-E(\epsilon_{\text{occupl}})\ , \tag{15}$$

where

$$E(\epsilon)=[(\epsilon-\lambda)^2+\Delta^2]^{1/2}\ , \tag{16}$$

with λ and Δ representing the Fermi level and the pairing gap, respectively, according to standard definitions and notation. The latter approach is adopted in the remaining discussions.

Best results (see below) for the proton separation energies were obtained with the following values for the central potential parameters: $V_0=50.6$ MeV, $r_0=1.250$ fm, $a=0.70$ fm, and $\kappa=0.86$. This r_0 value is 98% of the value listed in Table I as suggested by the $B(E2)\uparrow$ analysis. The neutron radius parameter was also taken as

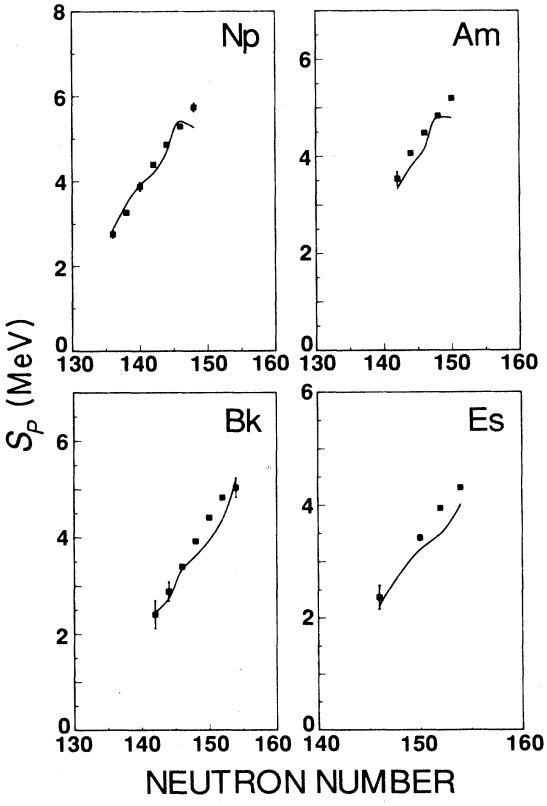

FIG. 6. Similar to Fig. 4, but for the proton separation energies (S_p) of selected actinide nuclei.

98% of the original value. The neutron separation energies led to the following recommended values for the neutron central potential parameters: $V_0=50.6$ MeV, $r_0=1.320$ fm, $a=0.70$ fm, and $\kappa=0.86$. (For the value of the neutron r_0 parameter, see also Sec. V.)

Figures 4 and 5 show a comparison of the separation energies of protons and neutrons, respectively, for several rare-earth nuclei. There is good overall correlation between the theoretical and experimental results. This correlation breaks down, however, for near-spherical nuclei (see the results in Fig. 4 for those Tb and Ho isotopes with $N\approx 82$). A similar, although less pronounced, discrepancy can be seen in Fig. 5 for the neutron separation energies of several $N\leq 83$ isotones. These nuclei were assumed to be spherical because the respective $(Z-1,N)$ or $(Z,N-1)$ core nuclei were calculated to be spherical. This assumption may not be entirely correct because one can argue that it is better to minimize the energy of the individual excited particles independently for each and every case. The discrepancy occurs at a rate near the magic number; this is precisely where the zero-point oscillations mentioned at the end of Sec. III become of some importance.

An analogous comparison for actinide nuclei is shown in Figs. 6 and 7. Here all the nuclei shown are known to be deformed in their ground states and the comparison can be considered very satisfactory given the simplifications mentioned at the beginning of this section.

V. SUMMARY AND CONCLUSIONS

The current global comparisons between the microscopic results based on the "universal" choice of the deformed Woods-Saxon potential and the extensive set of experimental data can be summarized as follows.

The $B(E2)\uparrow$ values calculated at the theoretical equilibrium deformations can be brought very close to the experimental values by reducing the original proton radius parameter (see Table I) by 2%. The final summary com-

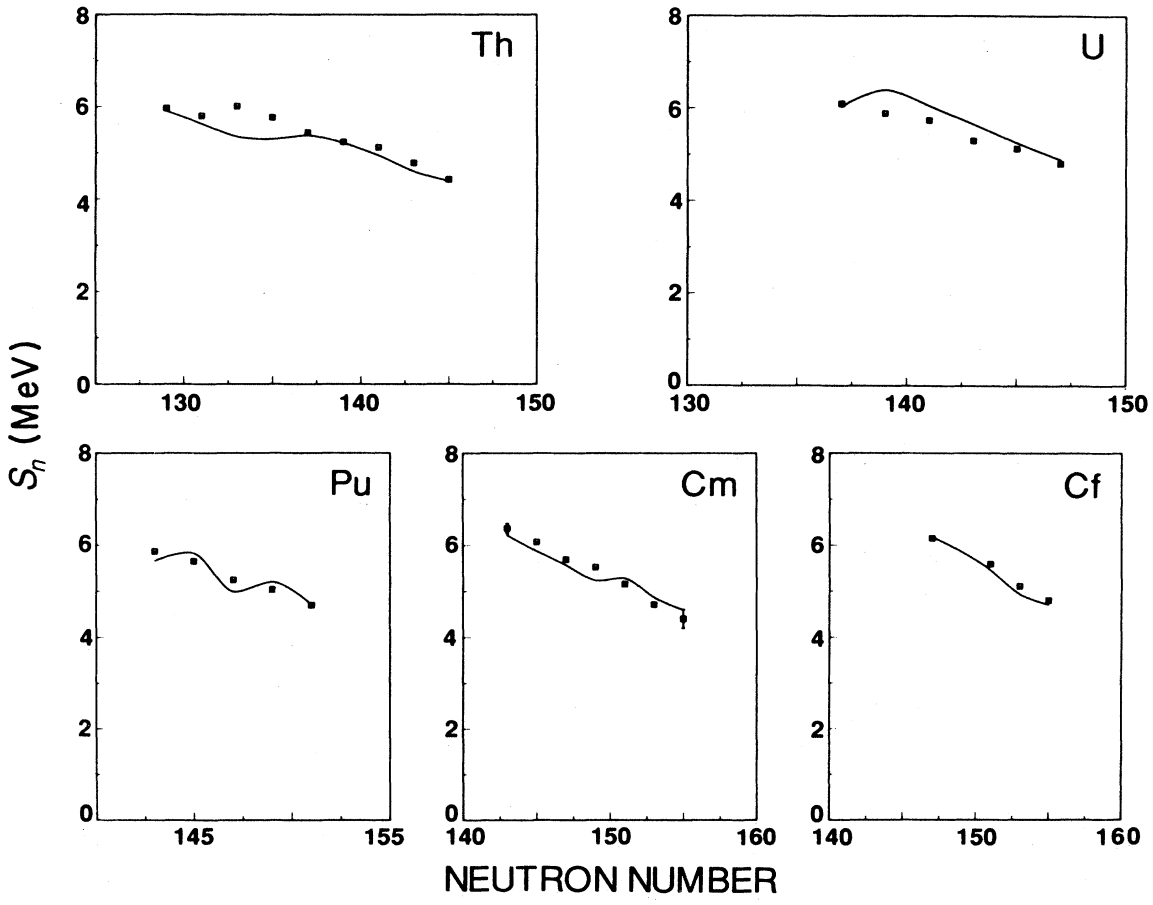

FIG. 7. Similar to Fig. 4, but for the neutron separation energies (S_n) of selected actinide nuclei.

parisons employing the original and reduced values are shown in Fig. 8. Two observations quickly emerge: (1) the discrepancies are small for the deformed nuclei, and (2) they are big in most cases when, at the same time, the uncertainties in the measured values are large.

Overall comparisons for the nucleon separation energies are shown in Fig. 9. Just as in the $B(E2)\uparrow$ case, large discrepancies are generally correlated with poorly known experimental values. It is also clear (less obviously from this figure but more strikingly from the near-zero points in Fig. 8) that near-spherical nuclei require a more careful treatment in the average field description.

The concept of the "universal" Woods-Saxon field appears to be well supported by the global comparisons made in this paper. Slight changes in the numerical values of some of the parameters are also warranted by the data. It is clear that even a small change in the proton radius parameter produces a noticeable systematic trend in the calculated $B(E2)\uparrow$ values. Even though a similar sensitivity is expected for the neutrons, the corresponding comparison with experiment would have to be less direct. It might be possible to employ the correlation between the neutron radius and the effective moment of inertia to improve, on the average, the quality of the pa-

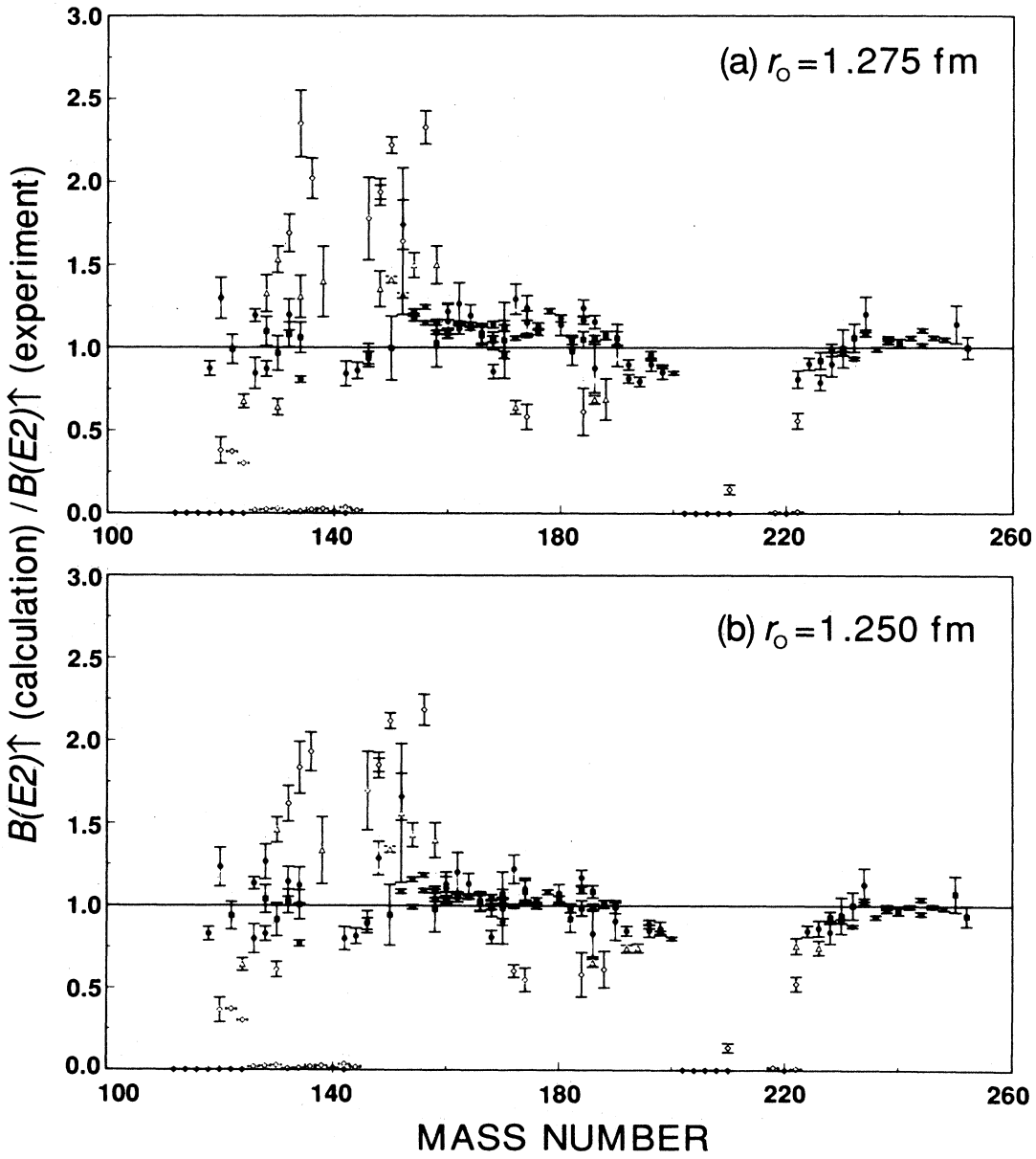

FIG. 8. Ratios of calculated to measured $B(E2)\uparrow$ values as a function of the mass number. The top figure was obtained with $R_0 = 1.275$ fm, the bottom with $r_0 = 1.250$ fm or 98% of the original value.

rametrization. By decreasing the neutron radius parameter to the same value as for protons, namely $r_0 = 1.250$ fm, one might be able to reproduce the so-called rigid-body moment of inertia values that are systematically overestimated when using the traditional neutron r_0 value of 1.347 fm. Of course, such a decrease will systematically change the binding energies as well. It is, however, a well-known property of the Schrödinger equation with potentials like the Woods-Saxon (and in the extreme case the square well) that by reducing the radius and increasing the potential depth one can preserve, on the average, the binding energies of the single-particle states. Such a test is in progress.[16]

ACKNOWLEDGMENTS

This research was supported in part by the U.S. Department of Energy under Contract No. DE-AS05-

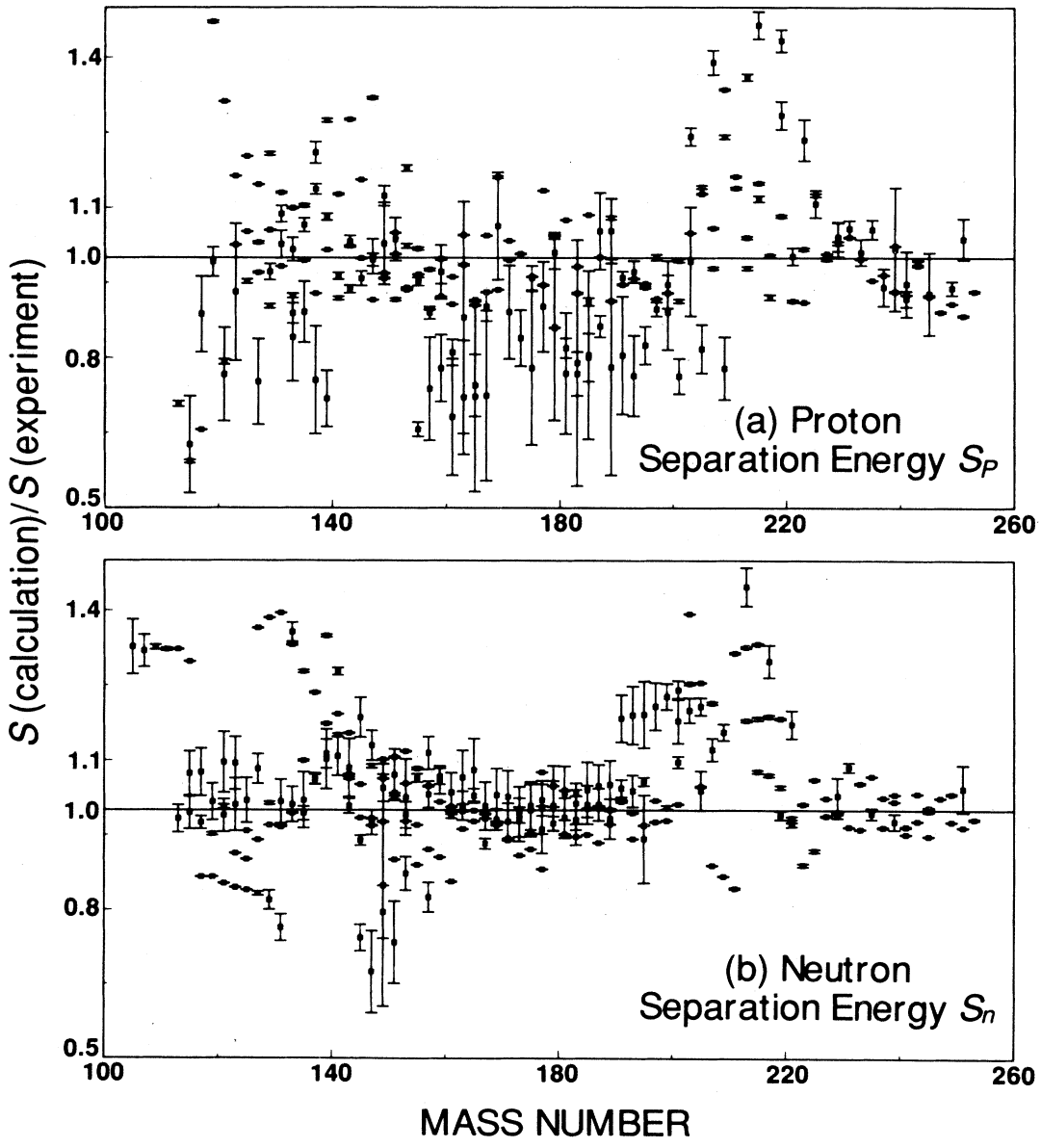

FIG. 9. Ratios of calculated to measured values of the separation energies for the last proton (S_p) or last neutron (S_n) as a function of the mass number.

76ERO-4936 with the University of Tennessee for the operation of the Joint Institute of Heavy-Ion Research and Contract No. DE-AC05-84OR21400 with Martin Marietta Energy Systems, Inc. for the operation of the Oak Ridge National Laboratory. The Joint Institute has as member institutions the University of Tennessee, Vanderbilt University, and the Oak Ridge National Laboratory.

[1]V. M. Strutinsky, Yad. Fiz. **3**, 614 (1966) [Sov. J. Nucl. Phys. **3**, 449 (1966)]; Nucl. Phys. **A122**, 1 (1968).

[2]For a review of the early applications, see, for example, M. Brack, J. Damgaard, A. S. Jensen, H. C. Pauli, V. M. Strutinsky, and C. Y. Wong, Rev. Mod. Phys. **44**, 320 (1972); H. C. Pauli, Phys. Rep. C **7**, 35 (1973). For more recent applications in high-spin nuclear phenomena, see, for example, J. Dudek, in *Proceedings of the International Conference on Nuclear Shapes, Crete, 1987,* edited by J. Garrett, C. A. Kalfas, G. Anagnostatos, E. Kossionides, and R. Vlastou (World Scientific, Singapore, 1988), p. 195; and S. Åberg, *ibid.*, p. 321.

[3]W. D. Myers and W. J. Swiatecki, Nucl. Phys. **81**, 1 (1966); P. Möller and J. R. Nix, Nucl. Phys. **A361**, 117 (1981); At. Data Nucl. Data Tables **26**, 165 (1981).

[4]For a discussion of the universal Woods-Saxon field in the high-spin and nuclear deformation context, see J. Dudek, in *Proceedings of the Winter Meeting in Nuclear Physics, Bormio, 1987,* edited by I. Iori (Ricerca Scientifica et Educazione Permanente, Milano, 1987), p. 554.

[5]S. Ćwiok, J. Dudek, W. Nazarewicz, J. Skalski, and T. Werner, Comput. Phys. Commun. **46**, 379 (1987).

[6]J. Dudek, Z. Szymański, and T. Werner, Phys. Rev. C **23**, 920 (1981).

[7]J. Dudek and W. Nazarewicz, Phys. Rev. C **31**, 298 (1985); J. Dudek, W. Nazarewicz, and N. Rowley, *ibid.* **35**, 1489 (1987).

[8]E. Rost, Phys. Lett. **26B**, 184 (1968).

[9]H. A. Bethe and J. Goldstone, Proc. Roy. Soc. London, Ser. A **238**, 551 (1957); H. A. Bethe, Annu. Rev. Nucl. Sci. **21**, 93 (1971). For a didactical review, see A. de Shalit and H. Freshbach, *Theoretical Nuclear Physics* (Wiley, New York, 1974), Vol. 1, p. 161.

[10]A. Bohr and B. R. Mottelson, *Nuclear Structure* (Benjamin, New York, 1969), Vol. 1, p. 218.

[11]J. Dudek, W. Nazarewicz, and T. Werner, Nucl. Phys. **A341**, 253 (1980).

[12]J. Dudek, A. Majhofer, and J. Skalski, J. Phys. G **6**, 447 (1980).

[13]S. Raman, C. H. Malarkey, W. T. Milner, C. W. Nestor, Jr., and P. H. Stelson, At. Data Nucl. Data Tables **36**, 1 (1987); S. Raman, S. Kahane, C. W. Nestor, Jr., and K. H. Bhatt, *ibid.* **42**, 1 (1989).

[14]S. Åberg, in *Proceedings of the International Conference on Nuclear Shapes, Crete, 1987,* edited by J. Garrett, C. A. Kalfas, G. Anagnostatos, E. Kossionides, and R. Vlastou (World Scientific, Singapore, 1988), p. 321.

[15]K. Bos, G. Audi, and A. H. Wapstra, Nucl. Phys. **A432**, 140 (1985).

[16]W. Nazarewicz (private communication).